

Article

An Operational Supporting System for Oil Spill Emergencies Addressed to the the Italian Coast Guard

Roberto Sorgente ^{1,†} , Dario La Guardia ² , Alberto Ribotti ^{1,*} , Marco Arrigo ² ,
Alessandro Signa ² , Federica Pessini ^{1,†} , Gennaro Oliva ³ , Andrea Pes ¹ , Angelo Perilli ¹ 
and Antonia Di Maio ^{4,†} 

¹ Institute for the Study of Anthropic impacts and Sustainability in marine environment (IAS), National Research Council (CNR), loc. Sa Mardini snc—Torregrande, 09170 Oristano, Italy; roberto.sorgente@cnr.it (R.S.); federica.pessini@ias.cnr.it (F.P.); andrea.pes@cnr.it (A.P.); angelo.perilli@cnr.it (A.P.)

² CInstitute for Educational Technology (ITD), National Research Council (CNR), 90146 Palermo, Italy; dario.laguardia@itd.cnr.it (D.L.G.); marco.arrigo@itd.cnr.it (M.A.); alessandro.signa@itd.cnr.it (A.S.)

³ Institute for High Performance Computing and Networking (ICAR), National Research Council (CNR), via Pietro Castellino 111, 80131 Napoli, Italy; gennaro.oliva@cnr.it

⁴ Institute of Anthropic impacts and Sustainability in marine environment (IAS), National Research Council (CNR), 00146 Rome, Italy; antonia.dimaio@cnr.it

* Correspondence: alberto.ribotti@cnr.it

† These authors contributed equally to this work.

Received: 23 November 2020; Accepted: 14 December 2020; Published: 19 December 2020



Abstract: Oil spill models are used to simulate the evolution of an oil slick that occurs after an accidental ship collision, malfunctioning of oil extraction platforms, or illegal discharges intentionally released by ships into the marine environment. We present an integrated operational oil spill prediction system that improves capacities in preventing and mitigating maritime risks from oil spills. The objective is to provide forecast information about the transport and the fate of a hypothetical oil spill under Nearly-Real Time hydrodynamic conditions in the western and central Mediterranean Sea. This complex forecast system is developed in the framework of the project SOS-Piattaforme & Impatti Off-Shore to the needs of Italian Coast Guard and other institutions, such as the Ministry of the Environment. This service has been operational since July 2020. The innovative aspect of this work is a graphical user interface (the GUI), which allows to select properties, time, and location of a potential oil spill and show the evolution of oil slick concentration and oil fate parameters. This platform represents the first component of a future Decision Support System aimed to identify the risk assessment of oil spills in order to better manage emergencies and minimize economic damages.

Keywords: oil spill; DSS; Graphical User Interface; emergency

1. Introduction

The evolution of an oil slick that occurs after an accidental ship collision or during oil extraction or other oil tanker activities produce a severe impact on the sea, in short and in long time, hitting biological, economic, political, cultural, and social matrices [1–4]. ITOPF [5] indicates that, in spite of a downward trend in the total number of accidental spill events, they are continuously reported in different regions of the world. At the same time, the operational pollution is increasing tending to be repetitive and chronic, so it is estimated that 45% of oil releases into the sea are due to illegal actions [6–11].

The Mediterranean Basin is very exposed to similar events due to the high maritime traffic, recording about 33% of the oil traffic in the world, 15% of the total maritime traffic and 10% of the heavy traffic. The exposure of the Italian seas is even higher due to important role of Italy as Europe's

largest refining center (about 80 million tons per year or about 1.6 millions of barrels per day—source: *Unione Petrolifera*, <https://www.unione petrolifera.it>), with its 11 refineries (9 coastal), 7 oil platforms, and 450 ports and terminals (14 for crude oil; <https://unmig.mise.gov.it>) [12,13] sited along the Italian peninsula and islands.

In the Italian seas, 131 accidents occurred from 1977 to 2010, 40% of which as load spill, with 160,000 tons of crude oil (mainly from the *Haven* accident), 5200 tons of gasoline, and 700 tons of fuel oil [14]. The most recent accidental oil spill was in October 2018 in the Liguro-Provençal basin, due to the collision between the Ro-Ro ship *Ulysse* and the container Ship CLS *Virginia*, impacting on the international protected marine area known as *Pelagos Sanctuary for Mediterranean Marine Mammals* [15,16].

It is then crucial for the Italian decision makers to have high quality information in near-real time about the numerical simulation of the transport and fate of the oil spills, to effectively manage the environmental crises. Due to this need and according to national laws (Italian DPCM 04 November 2010; DM 29 January 2013 of the Italian Environment Ministry; Italian D.L n. 145 of 18 August 2015) and International Conventions and Strategies for the protection of the sea (from the MARPOL 73/78 international convention to the Regional Strategy 2016–2021 of REMPEC), the Italian Ministry of the Environment and Protection of Land and Sea (MATTM) funded the project named *SOS-Piattaforme & Impatti Off-Shore* to have a system for the numerical forecasts of oil spills dispersion and fate in the Italian seas. The use of this system is exemplified thanks to a user-friendly Graphical User Interface (GUI) which guarantees a flexible approach and supports the Italian Coast Guard and MATTM in producing dynamical planning (i.e., upgradeable over time) of mitigation actions of the pollution event. This characteristic is decisive for a future development of a Decision Support System (DSS) able to produce efficient management solutions because it establishes the relation between the pollution event and the management requirements, while not replacing but supporting the decision makers [6,17–24]. *SOS-Piattaforme* will be described in the next sections: a complex set of coupled numerical models, composed by regional hydrodynamical models and an atmospheric one, will be introduced, followed by the description of an oil spill model and of the GUI developed ad hoc. Results of testing scenarios and conclusions will complete the paper.

2. Methods

The oil spill forecasting system (Figure 1) includes two main numerical modules and one GUI (Section 2.3).

The core of the system is the oil spill dispersion model (Section 2.1) which produces oil dispersion maps and trajectories, validated by drifter observations. This model is forced by the forecast sea currents and wind provided by the circulation module (Section 2.2). The latter consists of a Sub-Regional ocean forecasting system, forced in turn by means of a Weather Forecasting System and boundary conditions coming from a Regional ocean forecasting system. The whole *SOS-Piattaforme* system is used by the Italian Coast Guard by means of a GUI (Section 2.3), i.e., a user-friendly and simple interface which allows either to execute the simulations and visualize the results and validation reports. The information about the spilled oil can come from direct communications following the accident or from airplane/satellite data.

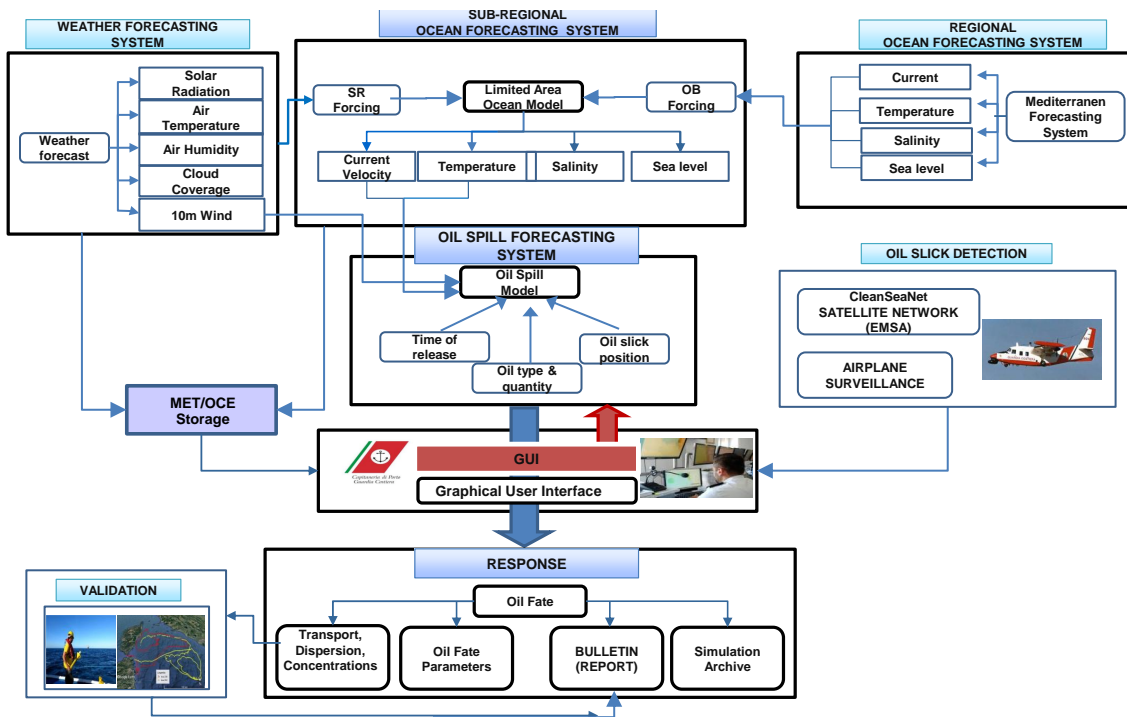


Figure 1. The figure shows the complex oil spill forecasting system, including the sub-regional ocean forecasting system, forced at the surface by heat and momentum fluxes using atmospheric parameters provided by the regional weather forecasting system, and at the boundary by the regional forecasting system. The graphical user interface (GUI), represented in Figure, is the tool to dialogue with such a system, which has as a result information about the transport and the fate of a hypothetical oil spill under Near-Real Time hydrodynamic conditions.

2.1. Oil Spill Dispersion Model

The oil spill transport and dispersion model is based on a Lagrangian particle tracking module named MEDSLIK_II [25,26]. The model predicts the evolution in time of the oil spill processes, including oil fate and concentrations, using the meteo-marine forcing inputs obtained by the operational circulation models (described in the next Section), as well the chemical-physical characterization of the oil. The model recognizes different oil types represented by °API, enough to cover the variety of physico-chemical properties.

The oil slick is represented into a set of initial adjacent particles and MEDSLIK_II calculates the advection-diffusion processes using a Lagrangian approach. The movement of the particles due to the currents, winds and turbulent diffusion is described by the Equation (1), where $\frac{\partial}{\partial t}$ is the time variation of the oil concentration (C) in a fixed point; $\vec{U}(\vec{x}, t)$ is the mean velocity:

$$\frac{\partial C}{\partial t} + \vec{U} \cdot \nabla C = \nabla(\vec{K} \cdot \nabla C) - \sum_{j=1}^M r_j(C). \tag{1}$$

The terms $r_j(C)$ are the M transformations rate, which induce the oil concentration due to chemical reactions and mixing [25] and $\vec{U} = \vec{U}_c + \vec{U}_w + \vec{U}_s$. In the past, the sea velocity current fields were provided by climatological (geostrophic currents, U_c) calculations [27], while, today, they are provided by the near real-time ocean forecasting system, as described in Section 2.2. Thus, the term $\vec{U}(\vec{x}, t)$ contains a rather satisfactory representation of the geostrophic currents (including also the Ekman currents, then the term \vec{U}_w can be neglect). However, it is sometimes necessary to also include the velocity correction term (\vec{U}_w) to better represent the effects of the local wind on the oil slick or as correction term, which takes into account hydrodynamic model errors [28]. It can be easily done by

the end-user through the GUI (see Section 2.3), setting the values of the drift factor (α) and the drift angle (β) of the following scalar equations:

$$U_w = \alpha(W_x \cos\beta + W_y \sin\beta), \quad (2)$$

$$V_w = \alpha(-W_x \sin\beta + W_y \cos\beta). \quad (3)$$

W_x and W_y are the wind velocities components (zonal and southern) at 10 m, respectively, provided by the weather forecast system (see Section 2.2). The last term (U_s) is the Stokes drift velocity, the currents wave-induced. Because the ocean forecasting systems are not coupled with wave models, we used the Stoke drift with the JONSWAP spectrum parameterization, which takes into account the wind amplitude and the fetch [29].

The forecast oil spill module provides the oil concentration and the hourly position of the oil at the surface, the evaporation and dispersion and the absorption of particles into the coastal environment. However, due to the complexity of the weathering processes which are represented by means of parameterizations [30–32], and uncertainty relating to slick movement, precise predictions of overall fate are still difficult to achieve. It is, therefore, important to understand the assumptions upon which weathering and trajectory models are based and to take these into account when analyzing the results. On the other hand, such models provide a useful indication in contingency planning processes because they give useful indication about the probable fate and behavior of a particular oil slick.

The coupling between the oil spill module and the meteo-oceanographic fields requires as inputs the wind forcing, the sea surface temperature, and the sea currents. These components are provided by the weather and ocean forecasting system described in the following section.

2.2. Ocean Circulation Models

The goal of this module is to provide reliable information and forecasts for marine environmental conditions at meso-scale in near-real time and boundary conditions to the oil spill module.

The hydrodynamic forecasting model is based on two limited area models (LAMs), named WMED60 and SCRM60, which represent the evolution of the Ocean Forecasting Systems developed during the projects PON-TESSA (Development of TEchnologies for Situational Sea Awareness, [33]) and MEDESS-4MS (Mediterranean Decision Support System Marine Safety) [34–36]. Both LAMs (Figure 2) are based on the Princeton Ocean Model (POM), a free-surface, sigma-coordinate (i.e., terrain-following) finite difference ocean model that solves the heat mass and momentum conservation equations of fluid dynamics [37]. POM has been widely used in the last two decades for studies of ocean dynamics [38–40] and operation purposes [36,41,42]. The model equations describe the three-dimensional velocity, temperature, salinity, and free surface fields assuming hydrostatic and Boussinesq approximation [43]. More details can be found in Mellor and Yamada [44], Ezer and Mellor [45], Mellor [46].

In this implementation the horizontal resolution for both ocean systems has been increased to $1/60^\circ$ (~ 2 km), in the vertical to 41 sigma layers, with a logarithmic distribution from the surface to the bottom. The aim was to enhance the forecasting skill of the systems through improved model resolution. Moreover, they use an innovative variational initialization technique (VIFOP) for its initial conditions and provides initial and boundary conditions to other coastal forecasting systems [47,48].

The WMED60 forecasting system, (Western Mediterranean intermediate Model) covering the Sardinia, the Ligurian and the Tyrrhenian seas from 30° N to 42° N and from 3° E to 16° E, while SCRM60 (Sicily Channel Intermediate Model) covers all seas around Sicily, between 32° N and 40° N and from 9° E to 17° E. The model bathymetry used is based on the U.S. Navy bathymetric database DBDB1 (1' horizontal resolution, ~ 2 km) and interpolated into the grid model by bilinear interpolation. The lowest depth is set to 10 m, to prevent crowding of sigma levels at the minimum depth resolved by the models. In addition, additional light smoothing is applied to reduce the sigma coordinate pressure gradient error [49] and to preserve most of the bathymetric details (Figure 2). Both hydrodynamic models do not include tides and the interaction between wave and current momentum.



Figure 2. Scheme of the computational domains of the limited area models (LAMs): the WMED6041 (red) and SCRM6041 (blue).

LAMs require appropriate data to define their initial and boundary conditions (IC and BC). For this purpose, the Mediterranean Forecasting System (MFS) regional model analysis and up to 10 days forecast were daily downloaded from the Copernicus Marine Information (marine.copernicus.eu). MFS assimilates satellite data and field measurements (XBTs, CTDs, Profiling Float). The model output of potential temperature, salinity and velocity fields are available with a horizontal resolution of $1/24^\circ \times 1/24^\circ$ (~ 4 km) and a vertical resolution of 141 unevenly levels [50]. These information are used to initialize and to downscale the numerical solution from regional to fine grid through an offline one-way asynchronous nesting, as described in Oddo and Pinardi [51].

During the numerical integration, both ocean LAMs are forced at the surface by heat and momentum fluxes using atmospheric parameters provided by the regional weather forecasting system named *Skiron* Kallos et al. [52]. It is a modified version of the regional Eta Model of the National Centers for Environmental Prediction (NCEP). The configuration used has a horizontal resolution of $1/20^\circ \times 1/20^\circ$ (~ 5 km) covering the whole Mediterranean basin, providing up to 120-h forecasts. The air-sea coupling assumes that the net shortwave and the downward radiation are provided hourly by *Skiron* itself, while momentum, heat, and water fluxes are carried out interactively, as the sea-surface temperature (SST) field required by the bulk formula is provided, for every time-step, by the model simulation. The evaporation flux is carried out interactively, while the precipitation is extracted from the weather forecast fields. Furthermore, the forecast of the atmospheric pressure is used to apply the inverse barometer correction to the surface elevation, as described by Wunsch and Stammer [53].

Processing Information

The forecast processing is based on a daily cycle for the production of ocean data (Figure 3). The forecast cycle is done each day (J), for the following 5 days. Each forecast is initialized at midnight from the downscaling of temperature, salinity, and velocity resulting from the simulation fields of the previous day ($J - 1$) and by the field from the following forecast day (J) of MFS. The forecast products of LAMs are updated daily at 18:00 UTC for the daily mean (averaged over a day, from midnight to midnight and centred at noon) and hourly (centred every half-hour) datasets. All the products are stored using the NetCDF format. The hourly forecast fields of superficial temperature and velocity are used to force the module of oil dispersion, described in the next paragraph.

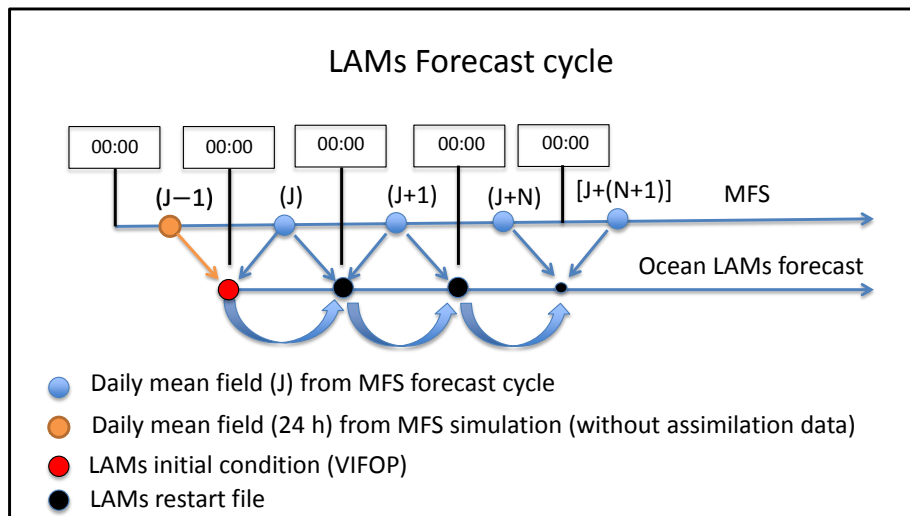


Figure 3. Every day (J) the ocean LAMs are initialized at midnight (the red circle) by variational initialization technique (VIFOP) using the simulation field (daily mean at J – 1, the orange circle) and the first forecast field (daily mean at J, the blue circle) from Mediterranean Forecasting System (MFS). These fields are centred at noon. The LAMs forecast is up to N (=5) days with output daily mean (centred at noon) and hourly (centred at half-hour).

2.3. The Graphical User Interface-GUI

The GUI allows a quick and simple interaction with the oil spill module to obtain information on transport and fate of an oil spill under near real time hydrodynamic conditions. It has been developed ad hoc in JAVA language and installed at CNR in Oristano. of Oristano. The access of the Coast Guard (hereafter end-user) to the GUI is allowed through credentials (*Username* and *Password*). Multiple users can simultaneously run their scenario of oil spill simulation; each simulation is queued waiting for the previous one to be completed and archived in a specified storage directory.

The required input data are entered in the GUI by the user (Figure 4); they are the initial time (UTC) and location of the oil spill, the estimated oil quantity and quality characteristics. The oil types are grouped in three oil classes (light, medium, heavy), according to their °API. Moreover, a list of the Italian oil platforms is also included, so their corresponding punctual geographical coordinates are automatically loaded according to the user’s choice. The oil spill dispersion forecast model runs up to 96 h and provides the temporal evolution of Oil Fate Parameters (see Section 3) and hourly images of the evolution of concentration. These images (see Section 3) contain a graphical representation of the hypothetical oil spill accident area, as well as the current field hourly averaged, the mean wind at the barycenter of the slick, and its horizontal dispersion, depicted by different colors (concentration).

The required input information and the output carried out from the oil spill forecast model are stored inside the server and available to the end-user.

Simulation

INPUT DATA
SIMULATION RESULTS AND REPORT

SIMULAZIONE

Simulation Name: Length of simulation (h): 72

Spill Type:

Platform List	Latitude	Longitude	Time (UTC)	Spill rate (tons/h)	Spill duration (h)	Volume (tons)
PREZIOSO	37° 0' 33"	14° 2' 42"	17/12/2020 15 PM	200	1	200

ChOOSE OFFSHORE

Operative

AQUILA

PERLA

PREZIOSO

ROSPO

SARAGO

UNCLASS

Oil Name:

Properties of Oil Ragusa

*API	19.8
Oil Density	0.935
Oil Residual Density	0.953
Oil Residual Percent	85.18
Oil Viscosity	77.0
Temperature at which Viscosity determined	38.0
Oil Vapour Pressure	0.25

SIMULATION SUMMARY

Simulation Name:

Length of simulation (h):

Ocean Forecasting:

Weather Forecasting:

Wave Forecasting:

*API:

Stokes drift:

Wind correction:

Depth of thermocline:

MAP

Start Simulation

1.0-alfa

Figure 4. The figure shows the customizable parameters of the GUI. In particular, in the first part the end user may choose the type of the simulation (spill type, length of simulation and eventually the platform with the relative coordinates); in the second part the chemico-physical parameters of the simulation, such as the oil type and its name. At the end, before starting the simulation, the end user can verify the settings in the summary of the simulation and on the map.

3. Results

At the beginning of a real environmental emergency several information that define the initial condition of the scenario, such as the geometry of the slick, the spilled quantity, the °API, etc., are not precisely known but estimated. Furthermore, since the atmospheric and marine circulation prediction models are subject to different approximations (mathematical and numerical), the realization of different scenarios, by varying the above inputs, become fundamental for the purpose of minimizing the environmental risk. Therefore, to verify the impact of the initial conditions on the evolution of the dispersion/concentration and transformation of an oil, known as Oil Fate Parameters (OFP), and the functioning of the GUI, some system tests were then carried out through the GUI assuming the same scenarios with different initial inputs. For simplicity, these tests were built in correspondence with the Prezioso oil platform in the Gulf of Gela (Channel of Sicily) at the sea surface. The tests are summarized in Table 1.

Table 1. The table summarizes the numerical experiments. The second column highlights the impact of the initial conditions on the evolution of the oil spill concentration and Oil Fate Parameters (OFP). The third column indicates the °API, the fourth the spill duration and the fifth the spill rate.

Exp	Parameters	°API	Spill Duration	Spill Rate
Exp. I (A)	Massive oil spill	19.8	Instantaneous	240 m ³ /h
Exp. II (B)	Wind drift term correction	19.8	Instantaneous	240 m ³ /h
Exp. III (C)	Continuous oil spill	19.8	24 h	10 m ³ /h
Exp. IV (D and E)	°API	37.8 and 10.7	24 h	10 m ³ /h

In the first experiment, the dispersion of 240 m³ of Ragusa oil (°API = 19.8) was simulated for the following 72 h, released instantly at 04:38 UTC on 05 May 2020. This is known as a massive spill and is usually due to accidents where a large amount of oil is dumped into the sea instantly (idealized scenario) or within hours. At the end of the numerical simulation, the GUI shows the temporal evolution of the OFP estimate (Figure 5A) and the oil concentration at the surface (Figure 6A). During the first 6 h of simulation, an increase in the evaporative component is due to the loss of the volatile component of the oil. Consequently, the fraction of oil dispersed into the sea tends to reduce by up to about 85%. The model shows just small impacts on the coast (beaching <1% after 30 h).

When larger impacts on the coast are possible, like in the previous experiment, and to reduce the uncertainty of the numerical solution of the integrated forecasting system, a second simulation was created also to evaluate the impact of the Wind Drift Correction term (see Equation (3)). Then the equations of the wind components were suitably modified ($\alpha = 0.03$ and $\beta = 20^\circ$). Although the wind intensity at the sea surface was increased by only 3%, the evolution of the OFP (Figure 5B) shows a significant different scenario compared with the previous experiment, also in terms of oil concentration (Figure 6B). Due to the increased speed of the surface current, the oil beaches in greater quantities; in fact after 40 h about the 60% of its initial volume reaches the coast. At the end of the numerical simulation (72 h) the fraction of evaporated oil is 20%, while that remaining at sea is reduced to 20% of the spilled volume.

By appropriately choosing the values of the alpha and beta parameters, through the GUI, the user can perform countless numerical scenarios with the aim of evaluating the time and place of the impact on the coast then minimizing the risk through the oil spill containment phase.

In a third experiment the impact of an oil spill characterized by a constant flow of low intensity, but which lasts over time, was evaluated. Generally this scenario occurs for releases from tanks or from the chest of a wreck bunker. Therefore, to simulate this new scenario through the GUI, we assumed a release of 240 m³ over 24 h. Compared with the second experiment, the model response still highlights the beaching process after 30 h but with an impact on the coast that only involves the 20% of the oil spilled (Figure 5C). This is due to the variability of the current which, during the oil-spill flow, modifies the distribution of the concentration (Figure 6C).

Another variable with an impact on the model solution, especially in terms of OFP, is the °API of the hydrocarbon. In the fourth experiment, the response of the model was then verified by selecting two different types of oil including an Arabian Light belonging to the lighter density class (°API = 37.8) and the heavy Katrina oil (°API = 10.7). The comparison between the OFPs (Figure 5D,E) shows a notable difference in evaporation rates which can reach 37% of the volume spilled with light oils, but only 10% with heavy oils. The high density of the Katrina oil ($\rho > 1$) induces its process of dispersion along the water column (Figure 5E), with a tendency to increase over time and reach approximately 20% after 72 h. Consequently, the percentages of oil beached on the coast and those present on the sea surface change.

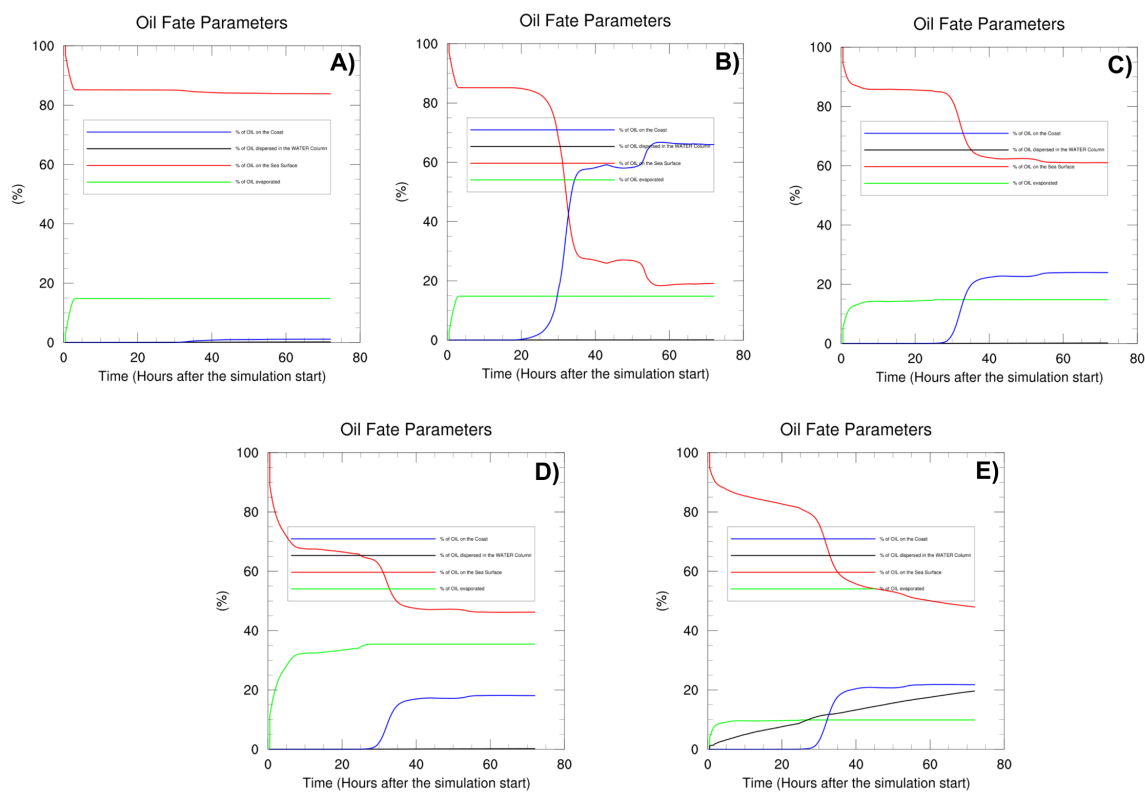


Figure 5. Temporal evolution (%) of the oil fate parameters during the 4 experiments from (A–E) characterized as in Table 1: the green line is the the evaporation, the red on is the oil on the sea surface, the blue one is the beaching, and the black one is the oil dispersed in the water.

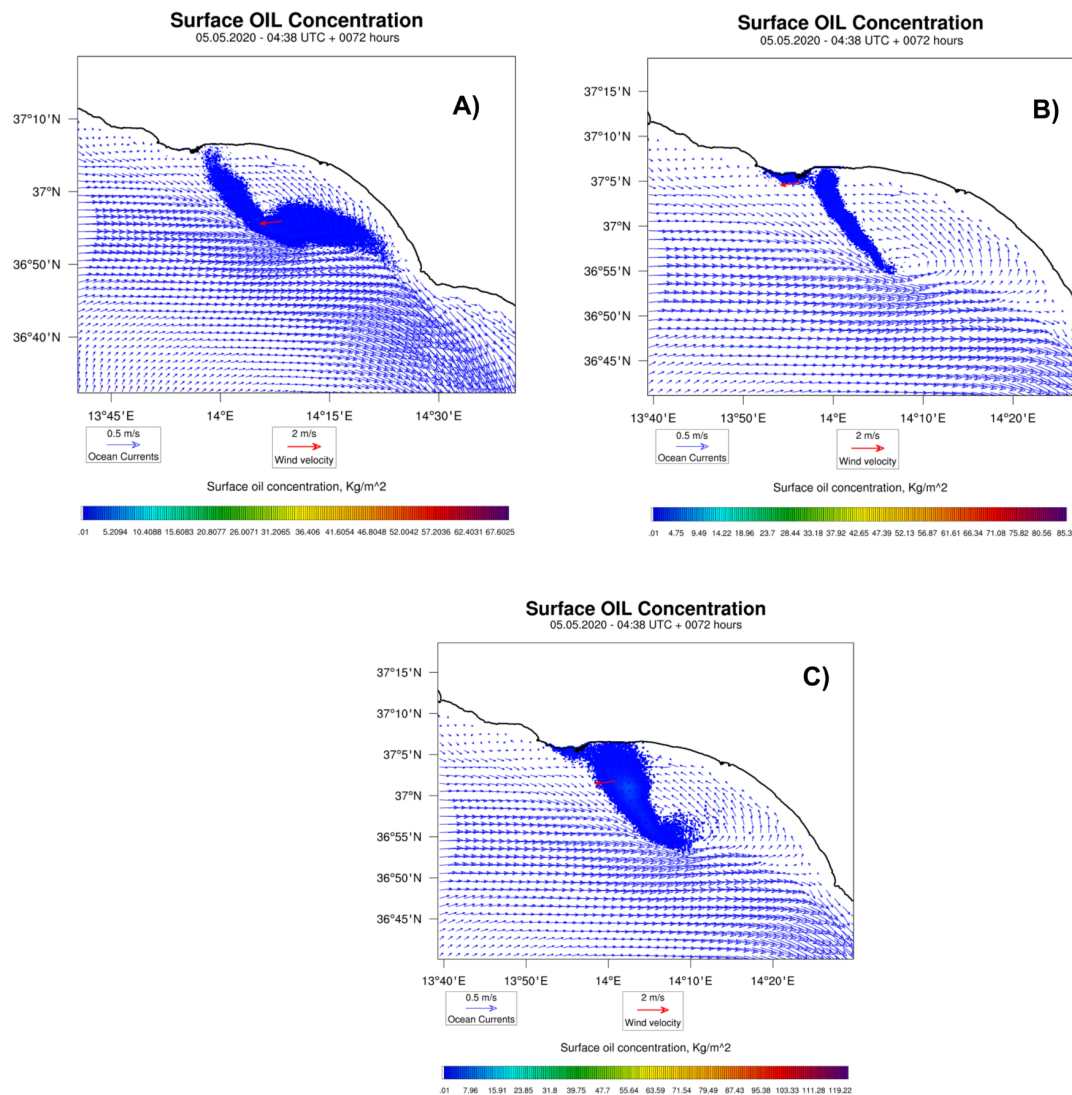


Figure 6. Forecast at 72 h of the oil concentration at the experiments with a massive oil spill (panel (A)), a wind drift term correction (panel (B)), and a continuous oil spill (panel (C)).

4. Discussion and Conclusions

This work has presented an oil spill prediction system, operational in the Western and Central Mediterranean Sea since July 2020 and used by the Italian Coast Guard and MATTM. The system is very complex and based on a marine circulation forecasting model coupled with an atmospheric one. Thanks to a very simple and user friendly interface, the GUI, the end users may dialogue with the oil spill prediction model, producing simulations of transport and fate of an oil spill under Nearly-Real Time hydrodynamic conditions. This kind of information may be very useful for planning the mitigation actions. By means of the GUI it is possible to realize in a simple way several different scenarios, in absence of precise details about the initial conditions, in order to reduce the uncertainties in the prediction. In fact, as demonstrated by the tests, the type of spill (massive or constant over time) can determine a significant difference in the concentration of oil-slick on the sea surface. This is due to the action of the spatial and temporal variability of the advection fields that act during the oil-spill modifying the oil concentration. Even the type of oil ($^{\circ}$ API) has a significant impact on the evolution of OFP, especially on the fraction that tends to evaporate ($^{\circ}$ API belonging to the light classes) and on that to disperse in the water column ($^{\circ}$ API belonging to the heavy class). Consequently, the fraction of oil that remains on the sea surface represents an estimate of

the initially dispersed percentage that should be recovered. Furthermore, close to the coast, or where the circulation is not adequately resolved by the hydrodynamic forecasting system, it is necessary to carry out further scenarios by correcting the numerical solution through the inclusion of the Wind Drift Correction term effect. This term, as previously seen, can considerably modify both the evolution of the OFPs (due to the occurrence of the beaching process) and the spatial distribution of the concentration.

The oil spill prediction system is actually used for real pollution emergencies, and also in case of antipollution exercises at sea, such as the recent one named *POLLEX2020*, coordinated by the Coast Guard to test their intervention readiness. Actually, the system takes partially into account two of the three hierarchical levels (*strategic* and *tactical*) of a DSS System (Figure 7), as described in Psafratsis and Ziogas [19] and Rademeyer and Lubinsky [54]. It provides an important support to identify the risk assessment of oil spills and may improve the management of the emergencies, minimizing the environmental and the economic damages.

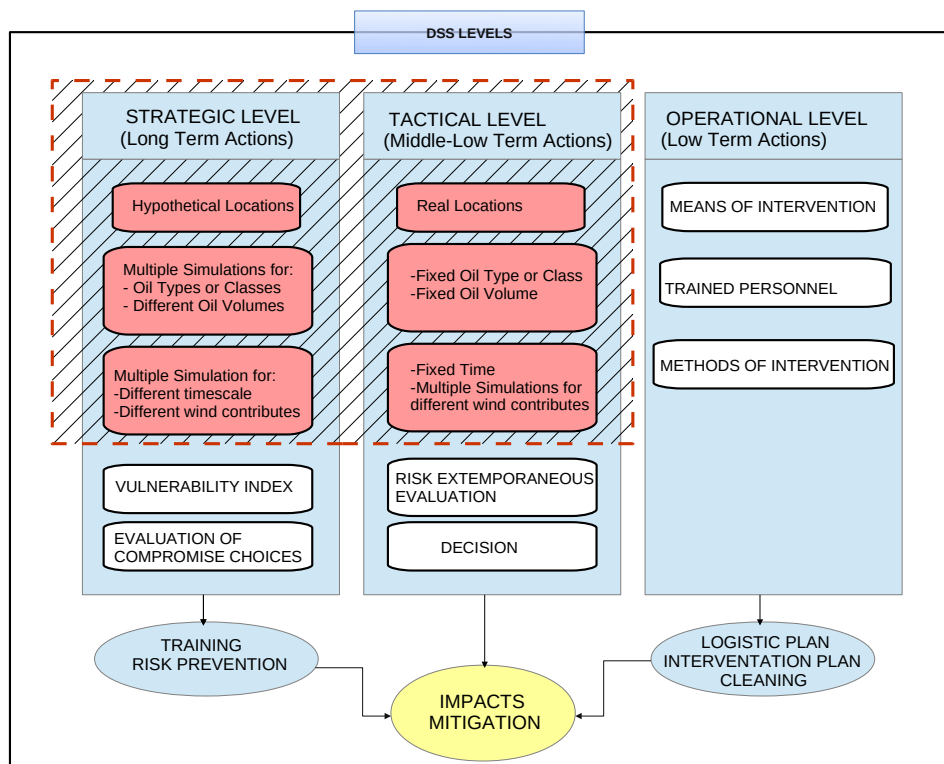


Figure 7. The GUI meets some points of the *strategic* and *tactical* levels of a Decision Support System (DSS) (red boxes in the dashed box). The active functions of the GUI (red boxes) allow to strongly minimize the response time of a decision making process in case of an oil spill emergency.

In the future, the modular design of the GUI will permit also to complete the tactical level, including a risk analysis scientific module dedicated to the probability of oil spill impacts. This will reduce much of the actual subjective component in the decision-making processes in the Italian seas.

Author Contributions: All authors contributed to the building of this paper in its different aspects. Conceptualization: R.S., A.R., and A.D.M.; Methodology: R.S., A.R., F.P., and A.D.M.; Software: A.P. (Andrea Pes), D.L.G., G.O., A.S., M.A.; Numerical Modeling: R.S., F.P., and A.D.M.; Writing—Original Draft Preparation: R.S., A.R., F.P., and A.D.M.; Writing—Review and Editing: R.S., A.R., F.P., D.L.G., G.O., A.S., M.A., A.P. (Angelo Perilli), and A.D.M. All authors have read and agreed to the published version of the manuscript.

Funding: The work is supported by the project SOS Piattaforme e Impatti Offshore (Servizio Di Previsione Numerica Della Dispersione Di Idrocarburi Dalle Piattaforme Petrolifere Del Canale Di Sicilia E Medio Basso Adriatico), funded by the Italian Ministry of the Environment and Protection of Land and Sea with Executive Agreement PNM.REGISTRO UFFICIALE.U 000939.17-01-2017 of 17.01.2017.

Acknowledgments: We thank the colleagues Fabio Antognarelli, Monica Pinna and Filippo Angotzi for their essential administrative support in Oristano for the management of the project.

Conflicts of Interest: The authors declare no conflict of interest.

References

1. Yuemen, D.; Adzigbli, L. Assessing the Impact of Oil Spills on Marine Organisms. *J. Oceanogr. Mar. Res.* **2018**, *6*. [CrossRef]
2. Juan, S.; Leonart, J. *Fisheries Conservation and Vulnerable Ecosystems in the Mediterranean Open Seas, Including the Deep Seas*; Technical Report; United Nations Environment Programme Mediterranean Action Plan Regional Activity Centre for Specially Protected Areas (RAC/SPA): Tunis, Tunisia, 2010; 103p.
3. Challenger, G.; Mauseth, G. Chapter 32—Seafood Safety and Oil Spills. In *Oil Spill Science and Technology*; Fingas, M., Ed.; Gulf Professional Publishing: Boston, MA, USA, 2011; pp. 1083–1100. [CrossRef]
4. Walker, A. Chapter 1—Oil Spills and Risk Perceptions. In *Oil Spill Science and Technology*, 2nd ed.; Fingas, M., Ed.; Gulf Professional Publishing: Boston, MA, USA, 2017; pp. 1–70. [CrossRef]
5. Roser, M. Oil Spills. Newblock Published Online at *OurWorldInData.org*. 2013. Available online: <https://ourworldindata.org/oil-spills> (accessed on 17 December 2020).
6. Moroni, D.; Pieri, G.; Tampucci, M. Environmental Decision Support Systems for Monitoring Small Scale Oil Spills: Existing Solutions, Best Practices and Current Challenges. *J. Mar. Sci. Eng.* **2019**, *7*, 19. [CrossRef]
7. Pavlakis, P.; Tarchi, D.; Sieber, A.; Ferraro, G.; Vincent, G. *On the Monitoring of Illicit Vessel Discharges: A Reconnaissance Study in the Mediterranean Sea*; Technical Report; Horizontal Services: Italy, 2001. Available online: https://ec.europa.eu/echo/files/civil_protection/civil/marin/reports_publications/jrc_illicit_study.pdf (accessed on 17 December 2020).
8. Tarchi, D.; Bernardini, A.; Ferraro, G.; Meyer-Roux, S.; Muellenhoff, O.; Topouzelis, K. Satellite monitoring of illicit discharges from vessels in the seas around Italy 1999–2004. *Eur. Comm.* **2006**.
9. Ferraro, G.; Bernardini, A.; David, M.; Meyer-Roux, S.; Muellenhof, O.; Perkovic, M.; Tarchi, D.; Tpozuelis, K. Towards an operational use of space imagery for oil pollution monitoring in the Mediterranean Basin: A demonstration in the Adriatic Sea. *Mar. Pollut. Bull.* **2007**, *54*, 403–422. [CrossRef] [PubMed]
10. Kirby, M.; Law, R. Accidental spills at sea—risk, impact, mitigation and the need for co-ordinated post-incident monitoring. *Mar. Pollut. Bull.* **2010**, *60*, 797–803. [CrossRef] [PubMed]
11. Pisano, A.; Dominicis, M.D.; Biamino, W.; Bignami, F.; Gherardi, S.; Colao, F.; Coppini, G.; Marullo, S.; Sprovieri, M.; Trivero, P.; et al. An oceanographic survey for oil spill monitoring and model forecasting validation using remote sensing and in situ data in the Mediterranean Sea. *Deep-Sea Res. II* **2016**, *133*, 132–145. [CrossRef]
12. Garcia, D.A.; Bruschi, D.; Cumo, F.; Gugliermetti, F. The Oil Spill Hazard Index (OSHI) elaboration. An oil spill hazard assessment concerning Italian hydrocarbons maritime traffic. *Ocean. Coast. Manag.* **2013**, *1*, 1–13. [CrossRef]
13. Farnesina. *The Italian Strategy in the Mediterranean—Stabilising the Crises and Building a Positive Agenda for the Region*; Technical Report; Farnesina-Italian Ministry of Foreign Affairs and International Cooperation: Rome, Italy, 2017.
14. Faticanti, M. *Sversamenti di Prodotti Petroliferi: Sicurezza e Controllo del Trasporto Marittimo*. Technical Report, ISPRA-Istituto Superiore per la Ricerca e la Protezione Ambientale. 2011. Available online: <https://www.isprambiente.gov.it/contentfiles/00010300/10390-rapporto-149-sversamenti-di-petrolio.pdf> (accessed on 17 December 2020).
15. REMPEC. *Pollution Preparedness and Response—Pollution Incidents Map*. Technical Report, Regional Marine Pollution Emergency Response Centre for the Mediterranean Sea (REMPEC). 2020. Available online: <https://www.rempec.org/en/our-work/pollution-preparedness-and-response/response/accident-map> (accessed on 17 December 2020).
16. Lyubartseva, S.; Smaoui, M.; Coppini, G.; Gonzalez, G.; Lecci, R.; Creti, S.; Federico, I. Model-based reconstruction of the Ulysse-Virginia oil spill, October–November 2018. *Mar. Pollut. Bull.* **2020**, *154*. [CrossRef]
17. Chang, N.B.; Wei, Y.; Tseng, C.; Kao, C.Y. The design of a gis-based decision support system for chemical emergency preparedness and response in an urban environment. *Comput. Environ. Urban Syst.* **1997**, *21*, 67–94.

18. Liubartseva, S.; Coppini, G.; Pinardi, N.; Dominicus, M.D.; Lecci, R.; Turrisi, G.; Creti, S.; Martinelli, S.; Agostini, P.; Marra, P.; et al. Decision support system for emergency management of oil spill accidents in the Mediterranean Sea. *Nat. Hazards Earth Syst. Sci.* **2016**, *16*, 2009–2020. [[CrossRef](#)]
19. Psafratsis, H.N.; Ziogas, B.O. A tactical decision algorithm for the optimal dispatching of oil spill cleanup equipment. *Manag. Sci.* **1985**, *31*, 1475–1491. [[CrossRef](#)]
20. Medini, P.C.P. A Spatial Decision Support System for Oil Spill Response and Recovery. Ph.D. Thesis, Arizona State University, Tempe, AZ, USA, 2018.
21. Amir-Heidari, P.; Raie, M. Response planning for accidental oil spills in Persian Gulf: A decision support system (DSS) based on consequence modeling. *Mar. Pollut. Bull.* **2019**, *140*, 116–128. [[CrossRef](#)] [[PubMed](#)]
22. Pourvakhshouri, S.; Shattri, B.M.; Zelina, Z.I.; Noordin, A. Decision support system in oil spill management. *Int. Arch. Photogramm. Remote Sens. Spat. Inf. Sci.* **2006**, *36*, 93–96.
23. Li, P. Development of an Integrated Decision Support System for Supporting Offshore Oil Spill Response in Harsh Environments. Ph.D. Thesis, Memorial University of Newfoundland, St. John's, NL, Canada, 2014. [[CrossRef](#)]
24. Martin, P.H.; LeBoeuf, E.J.; Daniel, E.B.; Dobbins, J.P.; Abkowitz, M.D. Development of a GIS-based. Spill Management Information System. *J. Hazard. Mater.* **2004**, *112*, 239–252.
25. De Dominicis, M.; Pinardi, N.; Zodiatis, G.; Lardner, R. A Lagrangian marine surface oil spill model for the short-term forecasting-Part I: Theory. *Geosci. Model Dev.* **2013**, *6*, 1851–1869. [[CrossRef](#)]
26. De Dominicis, M.; Pinardi, N.; Zodiatis, G.; Archetti, R. A Lagrangian marine surface oil spill model for the short-term forecasting-Part II: Numerical simulations and validations. *Geosci. Model Dev.* **2013**, *6*, 1871–1888. [[CrossRef](#)]
27. Al-Rabeh, A. Estimating surface oil spill transport due to wind in the Arabian Gulf. *Ocean. Eng.* **1994**, *21*, 461–465. [[CrossRef](#)]
28. Coppini, G.; De Dominicis, M.; Zodiatis, G.; Lardner, R.; Pinardi, N.; Santoleri, R.; Colella, S.; Bignami, F.; Hayes, D.R.; Soloviev, D.; et al. Hindcast of oil-spill pollution during the Lebanon crisis in the Eastern Mediterranean, July–August 2006. *Mar. Pollut. Bull.* **2011**, *62*, 140–153. [[CrossRef](#)]
29. Hasselmann, K.; Barnett, T.; Bouws, E.; Carlson, H.; Cartwright, D.; Enke, K.; Ewing, J.; Gienapp, H.; Hasselman, D.; Kruseman, P.; et al. *Measurements of Wind-Wave Growth and Sell Decay during the Joint North Sea Wave Project (JONSWAP)*; Technical Report; Deutschen Hydrographischen Zeitschrift: Hamburg, Germany, 1973 .
30. Mackay, D.; Paterson, S.; Trudel, K. *A Mathematical Model of Oil Spill Behavior*; Technical Report; University of Toronto: Toronto, ON, Canada, 1980.
31. Sutton, O.G. *Micrometeorology*; McGraw-Hill: New York, NY, USA, 1953.
32. Mackay, D.; Matsugu, R.S. Evaporation Rates of Liquid Hydrocarbon Spills on Land and Water. *Can. J. Chem. Eng.* **1973**, *51*, 434–439. [[CrossRef](#)]
33. Coppini, G.; Marra, P.; Lecci, R.; Pinardi, N.; Creti, S.; Scalas, M.; Tedesco, L.; D'Anca, A.; Fazioli, L.; Olita, A.; et al. SeaConditions: A web and mobile service for safer professional and recreational activities in the Mediterranean Sea. *Nat. Hazards Earth Syst. Sci.* **2017**, *17*, 533–547. [[CrossRef](#)]
34. Zodiatis, G.; De Dominicis, M.; Perivoliotis, L.; Radhakrishnan, H.; Georgoudis, E.; Sotillo, M.; Lardner, R.W.; Krokos, G.; Bruciaferr, D.; Clementi, E.; et al. The Mediterranean decision support system for marine safety dedicated to oil slicks predictions. *Deep Sea Res. Part II Top. Stud. Oceanogr.* **2016**, *133*, 4–20. [[CrossRef](#)]
35. Sorgente, R.; Tedesco, C.; Pessini, F.; De Dominicis, M.; Gerin, R.; Olita, A.; Fazioli, L.; Ribotti, A. Forecast of drifter trajectories using a Rapid Environmental Assessment based on CTD observations. *Deep Sea Res. II* **2016**, *133*, 39–53. [[CrossRef](#)]
36. Ribotti, A.; Antognarelli, F.; Cucco, A.; Falcieri, M.F.; Fazioli, L.; Ferrarin, C.; Olita, A.; Oliva, G.; Pes, A.; Quattrocchi, G.; et al. An Operational Marine Oil Spill Forecasting Tool for the Management of Emergencies in the Italian Seas. *J. Mar. Sci. Eng.* **2018**, *7*, 1. [[CrossRef](#)]
37. Blumberg, A.F.; Mellor, G.L. *A Description of a Three-Dimensional Coastal Ocean Circulation Model*; American Geophysical Union (AGU): Washington, DC, USA, 1987; pp. 1–16. [[CrossRef](#)]
38. Zavatarelli, M.; Pinardi, N.; Kourafalou, V.H.; Maggiore, A. Diagnostic and prognostic model studies of the Adriatic Sea general circulation: Seasonal variability. *J. Geophys. Res. Ocean.* **2002**, *107*, 2-1–2-20. [[CrossRef](#)]
39. Oddo, P.; Pinardi, N.; Zavatarelli, M. A numerical study of the interannual variability of the Adriatic Sea (2000–2002). *Sci. Total Environ.* **2005**, *353*, 39–56. [[CrossRef](#)] [[PubMed](#)]

40. Sorgente, R.; Di Maio, A.; Pessini, F.; Ribotti, A.; Bonomo, S.; Perilli, A.; Alberico, I.; Lirer, F.; Cascella, A.; Ferraro, L. Impact of Freshwater Inflow From the Volturno River on Coastal Circulation. *Front. Mar. Sci.* **2020**, *7*, 293. [[CrossRef](#)]
41. Onken, R.; Robinson, A.R.; Kantha, L.; Lozano, C.J.; Haley, P.J.; Carniel, S. A rapid response nowcast/forecast system using multiply nested ocean models and distributed data systems. *J. Mar. Syst.* **2005**, *56*, 45–66. [[CrossRef](#)]
42. Napolitano, E.; Iacono, R.; Sorgente, R.; Fazioli, L.; Olita, A.; Cucco, A.; Oddo, P.; Guarnieri, A. The regional forecasting systems of the Italian seas. *J. Oper. Oceanogr.* **2016**, *9*, s66–s76. [[CrossRef](#)]
43. Ezer, T.; Mellor, G.L. Diagnostic and prognostic calculations of the North Atlantic circulation and sea level using a sigma coordinate ocean model. *J. Geophys. Res. Ocean.* **1994**, *99*, 14159–14171. [[CrossRef](#)]
44. Mellor, G.; Yamada, T. Development of a turbulence closure model for geophysical fluid problems. *Rev. Geophys. Space Phys.* **1982**, *20*, 851–875. [[CrossRef](#)]
45. Ezer, T.; Mellor, G.L. A numerical study of the variability and the separation of the Gulf Stream induced by surface atmospheric forcing and lateral boundary flows. *J. Phys. Oceanogr.* **1992**, *22*, 660–682. [[CrossRef](#)]
46. Mellor, G. An equation of state for numerical models of oceans and estuaries. *J. Atmos. Ocean. Technol.* **1991**, *8*, 609–611. [[CrossRef](#)]
47. Drago, A.; Sorgente, R.; Ribotti, A. A high resolution hydrodynamic 3-D model simulation of the Malta shelf area. *Ann. Geophys.* **2003**, *21*, 323–344. [[CrossRef](#)]
48. Ribotti, A.; Bonomo, S.; Alberico, I.; Lirer, F.; Cascella, A.; Ferraro, L.; Sorgente, R. I-AMICA coastal hydrological surveys in the eastern Tyrrhenian Sea. *Seanoe* **2019**. [[CrossRef](#)]
49. Mellor, G.L.; Ezer, T.; Oey, L.Y. The pressure gradient conundrum of sigma coordinate ocean models. *J. Atmos. Ocean. Technol.* **1994**, *11*, 1126–1134. [[CrossRef](#)]
50. Clementi, E.; Pistoia, J.; Delrosso, D.; Mattia, G.; Fratianni, C.; Storto, A.; Drudi, M.; Grandi, A.; Ciliberti, S.; Lemieux-Dudon, B.; et al. *Mediterranean Sea Physics Analysis and Forecast (CMEMS MED-Currents 2015–2017)*; DataCite: Hannover, Germany, 2017. [[CrossRef](#)]
51. Oddo, P.; Pinardi, N. Lateral open boundary conditions for nested limited area models: A scale selective approach. *Ocean. Model.* **2008**, *20*, 134–156. [[CrossRef](#)]
52. Kallos, G.; Nickovic, S.; Jovic, D.; Kakaliagou, O.; Papadopoulos, A.; Missirlis, N.; Boukas, L.; Mimikou, N. The ETA Model Operational Forecasting System and its Parallel Implementation. In Proceedings of the Conference: Large-Scale Scientific Computation for Engineering and Environmental Problems, LSSC'97, Varna, Bulgaria, 7–11 June 1997; Vieweg: Kranzberg, Germany, 1997; Volume 62, pp. 176–188.
53. Wunsch, C.; Stammer, D. Atmospheric loading and the oceanic “inverted barometer” effect. *Rev. Geophys.* **1997**, *35*, 79–107. [[CrossRef](#)]
54. Rademeyer, A.; Lubinsky, D. A decision support system for strategic, tactical and operational visit planning for on-the-road personnel. *S. Afr. J. Ind. Eng.* **2017**, *28*, [[CrossRef](#)]

Publisher’s Note: MDPI stays neutral with regard to jurisdictional claims in published maps and institutional affiliations.



© 2020 by the authors. Licensee MDPI, Basel, Switzerland. This article is an open access article distributed under the terms and conditions of the Creative Commons Attribution (CC BY) license (<http://creativecommons.org/licenses/by/4.0/>).